Organic & Biomolecular Chemistry

ROYAL SOCIETY OF CHEMISTRY

PAPER

View Article Online
View Journal | View Issue

Cite this: *Org. Biomol. Chem.*, 2024, **22**, 3035

Identification and quantification of local antiaromaticity in polycyclic aromatic hydrocarbons (PAHs) based on the magnetic criterion†

Erich Kleinpeter *‡ and Andreas Koch

The spatial magnetic properties, through-space NMR shieldings (TSNMRSs, actually the ring current effect in ^{1}H NMR spectroscopy), of a selection of entirely antiaromatic and aromatic polycyclic conjugated hydrocarbons (PCHs), and aromatic PCHs with antiaromatic components, have been calculated using the GIAO perturbation method employing the nucleus independent chemical shift (NICS) concept and visualized as iso-chemical-shielding surfaces (ICSSs) of various sizes and directions. Using both in-plane and above/below-plane ICSS data, polycyclic aromatic hydrocarbons can be readily distinguished from polycyclic antiaromatic ones, even when antiaromatic components are present in the polycyclic aromatic hydrocarbons (PAHs). These antiaromatic zones can also be attributed to internal components of the in-plane deshielding belt present in aromatic compounds and possible partial antiaromatic ring current effects in the same place. This makes it possible to unequivocally confirm correctly assigned or adjust incorrectly assigned antiaromaticity of individual rings in the same molecule.

Received 21st January 2024,
Accepted 21st March 2024

DOI: 10.1039/d4ob00114a

rsc.li/obc

Introduction

The Hückel ($4n$ + 2) rule holds strictly only for monocyclic π-conjugated systems such as cyclopropenyl cation, benzene, cyclobutadiene, cyclopentadienyl cation and larger conjugated rings. Polycyclic aromatic hydrocarbons (PAHs) cannot comply with this rule, *e.g.* pyrene is aromatic despite its 16 π-electrons. It quickly became clear that the reason for pyrene's aromaticity is the 14 π-electrons of the conjugated perimeter of sp^2 hybridized carbon atoms: accordingly, within Platt's ring perimeter model[1] PAHs were divided into the perimeter and the inner core. Clar's π-sextet rule,[2] finally, regarded aromaticity of PAHs as a local property of six-membered rings. The aromatic π-sextets are localized in single benzene rings which are separated from adjacent rings by formal C–C single bonds; the more sextets can be found, the more stable and the more realistic should be the corresponding mesomeric descriptor of the PAH.[2] The required extended bond length analysis of the X-ray structures was conducted in 1996 by Paul von Ragué Schleyer who calculated Nucleus-Independent Chemical Shifts (NICSs) in the centre of the aromatic ring species [NICS(0)] and/or 1 Å above the centre [NICS(1)] and introduced these parameters as simple and efficient aromaticity probes;[3–5] later, and in addition, parts of the NICSs (*e.g.* NICS$_{\pi,zz}$ values) and NICS$_{\pi,zz}$ scans were introduced by Amnon Stanger[6–8] which consider only the π-proportion (σ-contributions do not have an effect on ring currents) and improved the accuracy of the aromaticity statement based on the magnetic criterion.

In proton NMR spectroscopy, the *ring current effect of aromatic compounds* (generally: the *anisotropy effect* of functional groups) proves to be a useful tool in assignment procedures: protons positioned stereochemically *above*/*below* the benzene ring plane are high field, and *in-plane* ones are low field shifted. The initially calculated causative ring current and the effect on proton chemical shifts in ^{1}H NMR spectra determined by Pople and Untch,[9] could be later visualized by Herges *et al.*[10] using the Anisotropy of the Induced Current Density (ACID) method by vector maps (vectors indicate direction and intensity of the in-plane current and contours/shading the total magnitude); anticlockwise (clockwise) circulations represent paratropic (diatropic) ring currents. Comparable models to quantify and visualize electron delocalization have been developed by Dickens and Mallion[11] and Sundholm *et al.*[12] Pioneering works for developing the theoretical study of the ring current have been carried out by Todd Keith and Richard Bader.[13]

Universität Potsdam, Institut für Chemie, Karl-Liebknecht-Str. 24–25, D-14476 Potsdam (Golm), Germany. E-mail: ekleinp@uni-potsdam.de, Andreas.Koch@uni-potsdam.de

†Electronic supplementary information (ESI) available: Detailed TSNMRS data of PAHs studied in the paper and the corresponding data of a few others. See DOI: https://doi.org/10.1039/d4ob00114a

‡The authors declare equal participation.

The relationship of NICSs and ring currents for evaluating aromaticity, Current Density Analysis (CDA) and $NICS_{\pi,zz}$ (single value or scan), has been studied by Fowler's and Stanger's groups[14] and the consensus was found to be surprisingly high, considering the differences between the methods.[14]

Polycyclic conjugated hydrocarbons (PCHs) often have unique optoelectronic and supramolecular properties and, therefore, are often found as components of organic electronics such as light emitting diodes, transistors and photovoltaic cells. Structure elucidation is carried out by single crystal X-ray analysis. Beside the photophysical properties (UV–vis absorption and emission spectra) and related QC calculations to get information about the HOMO–LUMO gap, the (anti)aromaticity of individual rings of the PCHs is evaluated by performing a NICS analysis, usually [$NICS(1)_{\pi,zz}$], based on the crystal structure. Based on the $NICS(1)_{\pi,zz}$ values aromatic, non-aromatic and antiaromatic rings are identified and, as support, very often the ACIDs are calculated and the clockwise (diatropic) and counter-clockwise (paratropic) ring currents are compared with $NICS(1)_{\pi,zz}$ values or scans to verify the identity. The final information obtained is existing aromaticity ($-NICS_{\pi,zz}$ values), antiaromaticity ($+NICS_{\pi,zz}$ values), and local/global/peripheral dia- and para-tropic ring currents, respectively.

But NICS analysis (in all its versions) of individual rings in multi-ring systems contains contributions from all induced magnetic fields including contributions from adjacent induced ring currents. Thus, local aromaticity has no special chemical meaning and Stanger argues that the term "local aromaticity" should not be used for multi-ring systems,[14b] because (anti)aromaticity of PCHs is not easily defined, especially in compounds with dominant diatropic currents (local and/or global) which contain only small counter-paratropic current loops.

Ring currents (employing the corresponding tools) can be visualized and the strength measured as well; the NICS index (in all its versions) is an experimentally unavailable quantity of aromaticity.[3,4] However NICS values on a grid around (anti)aromatic structures (spatial NICS)[15] can be computed as Through-Space NMR Shieldings (TSNMRSs) and visualized as Iso-Chemical-Shielding-Surfaces (ICSSs).[16] This TSNMRS grid has been successfully employed to qualify and quantify the ring current effect in the ^{1}H NMR spectra of (anti)aromatic moieties.[16] Because there are continuing reservations[17,18] about quantifying molecular response properties by an unobservable quantity such as NICSs,[19] we were able to prove that spatial NICSs (TSNMRSs) can successfully assign the stereochemistry of structures,[20–23] even preferred conformers in dynamic processes still fast on the NMR timescale.[20] Hence, the *experimentally measurable ring current effect Δδ/ppm* in ^{1}H NMR spectra proves to be the *molecular response property of TSNMRS (spatial NICS)*.[20–23] Consequently, we have a method[15,16,22] in hand which precisely visualizes and qualifies (anti)aromaticity based on the magnetic criterion[22] and proves useful for the intended magnetic characterization of PCHs.

The basic usability of our concept of spatial NICSs (TSNMRSs) was not only applicable for successfully corroborating or predicting experimental NMR studies but also for the general re-evaluation and classification of reactive species such as for example carbenes[24] and carbones,[25] and it lends itself to the basic assessment of corresponding chemical issues.

Also a 3D isotropic magnetic shielding contour plot method for contorted PAHs has been published recently.[26]

Computational details

The quantum chemical calculations were performed using the Gaussian 09 program package[27] and carried out on LINUX clusters. The studied structures (in Fig. 1–5) were fully optimized at the MP2/6-311G(d,p) level of theory without constraints.

NICS values[4,5] were computed on the basis of MP2/6-311G (d,p) geometries using the gauge-independent atomic orbital (GIAO) method[28] at the B3LYP/6-311G(d,p)[29–31] theory level.[32] To calculate the spatial NICSs, ghost atoms were placed on a −10 Å to +10 Å lattice with a step size of 0.5 Å in the three directions of the Cartesian coordinate system. The zero points of the coordinate system were positioned at the centers of the studied structures. The resulting 68 921 NICS values, thus obtained, were analyzed and visualized by the SYBYL 7.3 molecular modeling software;[33] different iso-chemical-shielding surfaces (ICSSs) of −0.5 ppm (orange) and −0.1 ppm (red) *deshielding*, and 5 ppm (blue), 2 ppm (cyan), 0.5 ppm (green) and 0.1 ppm (yellow) *shielding* were used to visualize the TSNMRS of the studied structures. ICSSs are a quantitative indication of the diatropic or paratropic ring current effect in

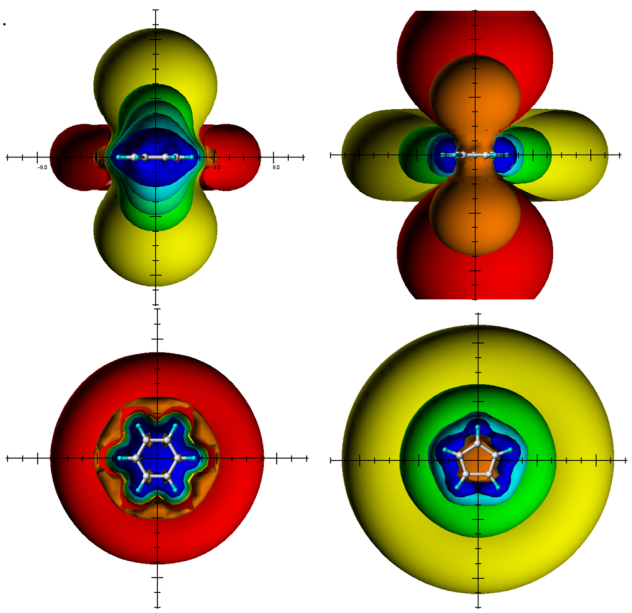

Fig. 1 Benzene **1** (left; side and top view) and cyclopentadienyl cation **2**, the prototypes of 6π-aromaticity and 4π-antiaromaticity; visualisation of TSNMRSs by different ICSSs of −0.5 ppm (orange) and −0.1 ppm (red) *deshielding* and 5 ppm (blue), 2 ppm (cyan), 0.5 ppm (green) and 0.1 ppm (yellow) *shielding*.

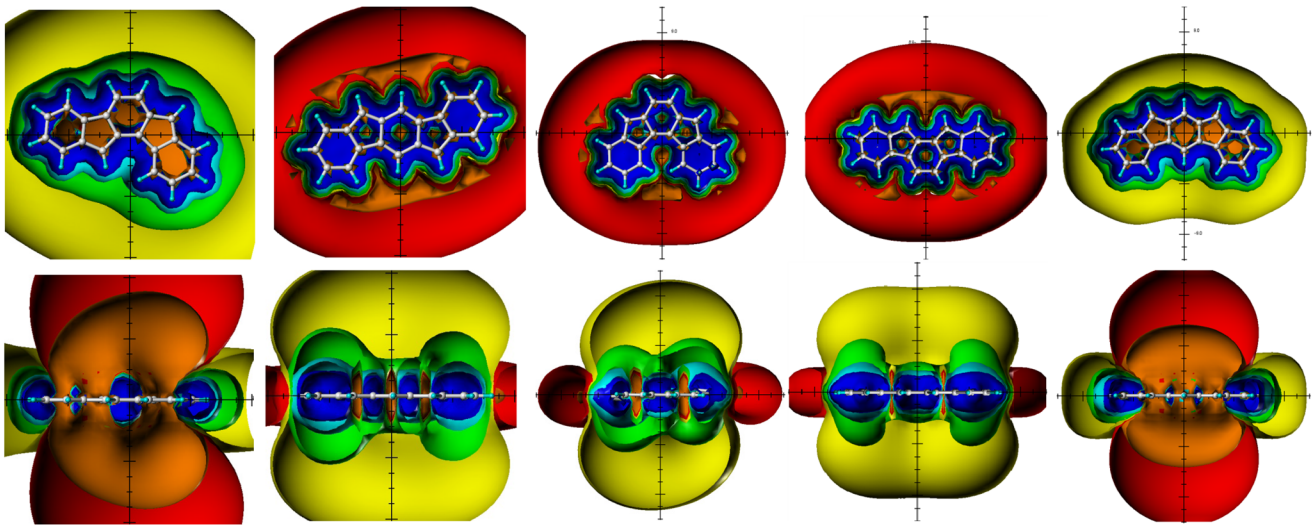

Fig. 2 TSNMRSs of the benzofused 20π-indenofluorene regioisomers, from left, **3** (indeno[1,2-*a*]fluorene), **4** (indeno[1,2-*b*]fluorene), **5** (indeno[1,2-*c*]fluorene), **6** (indeno[1,2-*a*]fluorene) and **7** (indeno[1,2-*b*]fluorene); visualisation of TSNMRSs (above, top view; below, side view) by the different ICSSs of −0.5 ppm (orange) and −0.1 ppm (red) *deshielding* and 5 ppm (blue), 2 ppm (cyan), 0.5 ppm (green) and 0.1 ppm (yellow) *shielding*.

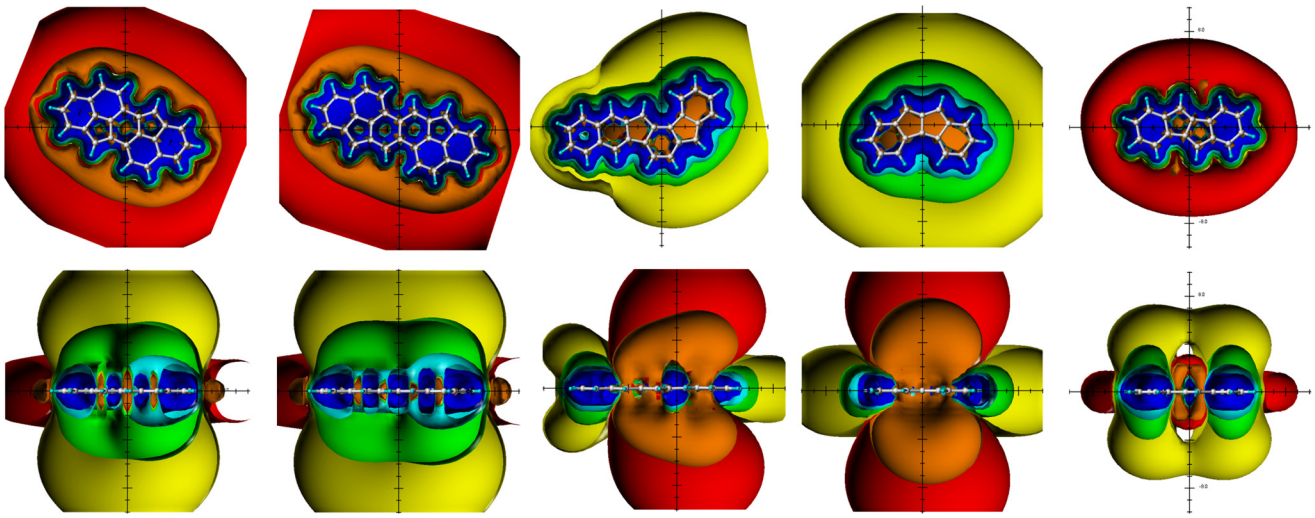

Fig. 3 TSNMRSs of, from left, the 24π-electron cyclopenta[*pqr*]indeno[2,1,7-*ijk*]tetraphene (**9**) and the 28π electron cyclopenta[*pqr*]indeno[7,1,2-*cde*]picene **10**, the 16π-electron benzofused indeno[1,2-*a*]fluorene **8**, the dibenzo[*a*,*f*]pentalene **11**, and dibenzo[*a*,*e*]pentalene **12** (above, side view; below, top view); visualization by different ICSSs of −0.5 ppm (orange) and −0.1 ppm (red) *deshielding* and 5 ppm (blue), 2 ppm (cyan), 0.5 ppm (green) and 0.1 ppm (yellow) shielding.

^{1}H NMR spectroscopy;[15,16,22] the closer the distance (in Å) of a certain *shielding (deshielding) ICSS* to the center of the molecules, the stronger the corresponding ring current effect which is measurable as $\Delta\delta(^1\text{H})$/ppm in ^{1}H NMR spectroscopy.

Results and discussion

Ring current effects of benzene and cyclopentadienyl cation (CPDC) as references

The ring current effects of benzene and CPDC are due to the present diatropic and paratropic ring currents, respectively, very diagnostic for the present aromaticity and antiaromaticity, respectively (Fig. 1). The ring current effects of both molecules show opposite signs and are therefore particularly easy to distinguish based on their ICSSs with regard to their aromaticity (shielding above/below the plane, deshielding in-plane) and antiaromaticity (deshielding above/below the plane, shielding in-plane). In the following text we use for this reason both ring current effects as a reference for aromaticity and antiaromaticity present in the investigated PCHs, although the underlying ring currents are only determined by the direction and size of the π loops, but the corresponding ring current effects represent sum parameters that contain further effects, especially

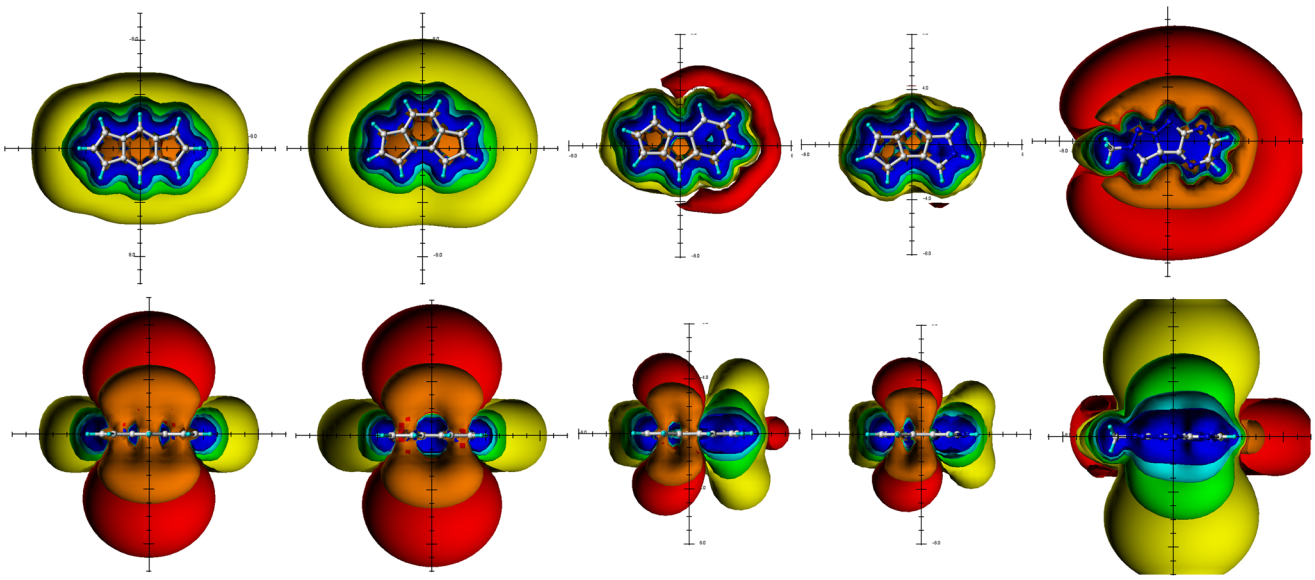

Fig. 4 TSNMRSs of, from left, *s*-indazene **13**, *as*-indazene **14**, a stable 12π benzo-pentalene **15**, pentaleno[1,2-*c*]pyrrole **17** and the zwitterionic polyazapentalene **16** (above, side view; below, top view); visualisation by different ICSSs of −0.5 ppm (orange) and −0.1 ppm (red) *deshielding* and 5 ppm (blue), 2 ppm (cyan), 0.5 ppm (green) and 0.1 ppm (yellow) *shielding*.

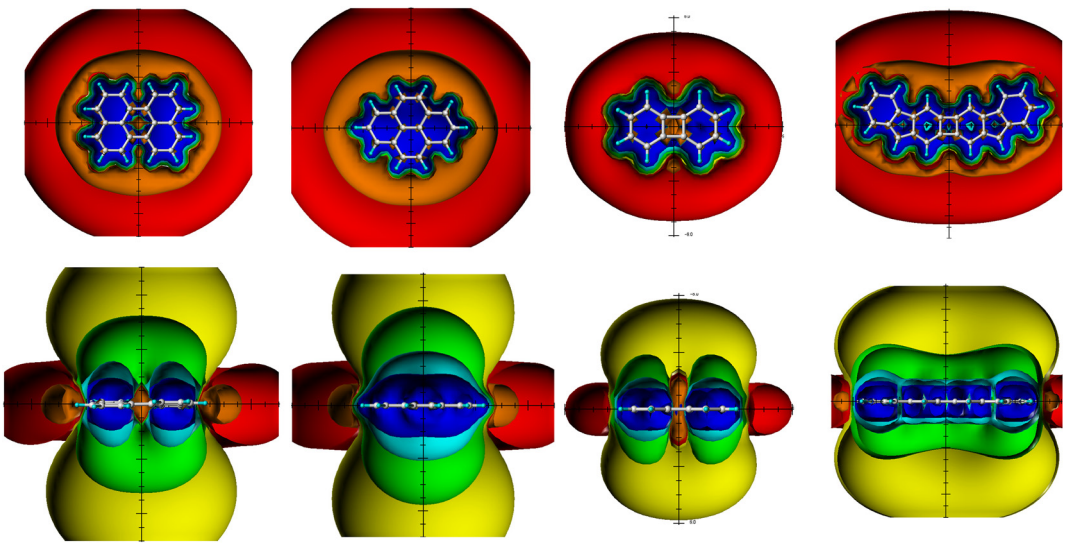

Fig. 5 TSNMRSs of, from left, perylene **19**, pyrene **20**, biphenylene **18** and the stable 24π diindeno[2,1-*b*:2′,1′-*h*]biphenylene **21** (above, side view; below, top view); visualisation by different ICSSs of −0.5 ppm (orange) and −0.1 ppm (red) *deshielding* and 5 ppm (blue), 2 ppm (cyan), 0.5 ppm (green) and 0.1 ppm (yellow) *shielding*.

σ components and ring current effect shares of neighboring rings.

Aromaticity/antiaromaticity of the bis-benzo-annelated indenofluorene regioisomers and analogues

The indenofluorene regioisomers (Scheme 1) each contain 20π electrons and thus are fully antiaromatic according to Hückel's rule.[34] However, when being studied and characterized by the NICS parameter it was found out surprisingly that only two of them are antiaromatic (**3** and **7**), the remaining three regioisomers prove to be proaromatic (**4**–**6**).[34] Generally, paratropicity of the indacene core and diatropicity of the outer benzenes were found for the latter group, and, in addition, the antiaromatic indenofluorenes receive more resonance stabilization energy in the diradical form and thus show greater diradical character.[35] Also the ^{1}H chemical shifts at high field of the protons of the antiaromatic regioisomers were employed as hints to the present antiaromaticity.[36]

The spatial magnetic properties (actually the ring current effects) of the benzofused 20π-indenofluorene regioisomers

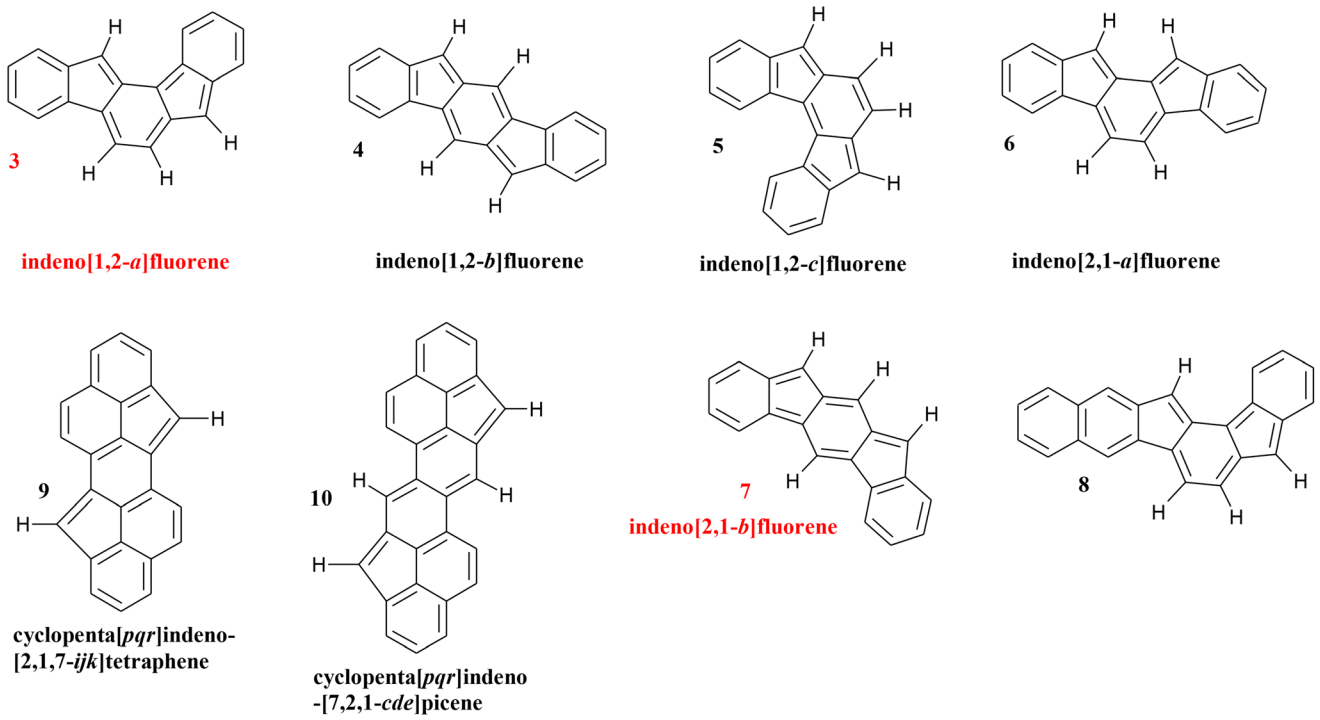

Scheme 1 Structures of the indenofluorene regioisomers (**3–7**, antiaromatic in red) and the π-extended and curved analogues (**8–10**).

are given in Fig. 2. Both groups of the regioisomers can be readily distinguished: the antiaromatic representatives **3** and **7** indicate the present antiaromaticity by the paratropic ring current effects (deshielding above/below and shielding in plane), the remaining three regioisomers are aromatic PCHs and are most clearly recognized by the deshielding belt. While in the antiaromatic analogues **3** and **7** both deshielding ICSSs above/below the plane and the shielding ICSSs in plane are closed and completely intact, the diatropic ring current effects of the aromatic regioisomers (shielding ICSS above/below the plane) **4–6** are accompanied by paratropic areas (deshielding above/below plane); only the deshielding belt (in plane deshielding ICSSs) remains completely intact and classifies unequivocally these three compounds as PAHs. The paratropic areas within the indenofluorene core of the aromatic regioisomers can be discussed in two ways: (i) as inner parts of the deshielding belts of the dominant diatropic ring current effects or (ii) as indications of weak counter-paratropic current loops in the ring members of the indofluorene core. The latter interpretation is usually the result of NICS studies: only individual NICS values and/or the corresponding NICS values along a scan are available for evaluation; there is no information from the existing deshielding belts of the diatropic ring current effect that should be included necessarily in the interpretation.

These internal contributions are more intense than in the external aromatic deshielding belt and for this reason should be addressed as antiaromatic contributions of the indenofluorene core of the PAHs.

The indeno[1,2-*a*]fluorene regioisomer **3** is still unknown but its antiaromaticity is completely clear from the spatial magnetic properties reported in this paper. The aromaticity of PAH **4**, the basic structure of a number of synthesized indeno[1,2-*b*]fluorenes and assigned as formally antiaromatic,[37] proves to be unequivocal now and misattributions can be excluded;[37] Haley's group already found through an NICS(1)$_{xy}$ scan study the very slightly paratropic indacene core and the aromaticity of the outer rings,[37,38] and assigned the associated ring currents.[39] They came to the same result for regioisomer **5**;[37,38] which we could confirm through the present TSNMRS study. Substituted indeno[2,1-*a*]fluorenes **6** and [2,1-*b*]-analogues **7** were synthesized by the group of Yoshito Tobe;[40,41] while aromaticity of the terminal benzene rings and an antiaromatic central indazene moiety in **6** was identified,[40] the antiaromaticity of **7** was not noted but a moderate contribution of a biradical canonical structure to the ground state electronic configuration was proved by ESR.[41]

These partly uncertain results on the (anti)aromaticity of the indeno[1,2-*a*]fluorene regioisomers, which resulted from various NICS value and/or NICS scan studies, were confirmed, unified and merged by the present calculations of the spatial magnetic properties. Hereby, the inclusion of the shielding/deshielding belts in the plane of the planar (anti)aromatic hydrocarbons, respectively, was particularly valuable.

It is worth mentioning that the found aromaticity/antiaromaticity of the regioisomers is in complete accordance with Clar's rule:[2] the two π-sextets in the aromatic regioisomers **4–6** and **8** are sufficient to introduce aromaticity, one π-sextet in **3**

and **7** proves to be inadequate and the less stable antiaromatic PCHs remain.

The 24- and 28-π-electron analogues, namely, cyclopenta[*pqr*]indeno[2,1,7*ijk*]-tetraphene (**9**) and cyclopenta[*pqr*]indeno[7,1,2-*cde*]picene (**10**) (Scheme 1) were synthesized and further studied by NICS calculations by the group of Xinliang Feng in Dresden.[42] They obtained results which are in accordance with an antiaromatic nature of **9** and **10** and the two PCHs having rings with different degrees of net aromatic or antiaromatic nature.[42] In the five- and six-membered rings in the central regions Feng *et al.*[42] found paratropic currents to be dominant, in the peripheral moieties are patterns common for nonaromatic and antiaromatic entities.[42]

The TSNMRS visualizations of **9** and **10** in Fig. 3 display not much different spatial magnetic properties than the aromatic indenofluorene regioisomers (**4–6** and **8**). Like the latter group, **9** and **10** prove to be PAHs with possible weak counter-paratropic current loops in the ring members of the indofluorene core and dominant diatropic ring currents along the peripheral moieties. However, the inner ICSS(−0.5) and ICSS(−0.1) in **9** and **10** are of about same size as the outer ICSSs of the deshielding belt of these PAHs. This observation suggests that the inner indenofluorene core is non-aromatic rather than slightly anti-aromatic. On the other hand, **8**, with addition of another annelated phenyl ring to the 20π-indenofluorene regioisomer **4**, is insufficient to tilt the antiaromaticity of **3** towards aromaticity (Scheme 1 and Fig. 3): the antiaromaticity in **8** as in **4** remains, only the antiaromatic shielding belt around the additional phenyl ring proves to be slightly extended and indicates an existing very weak counter-diatropic current loop in the additional phenyl ring; this is also due to the still only one π-sextet in **8** in complete accordance with the Clar rule.[2] Benzannelation of the indeno[1,2-*b*]fluorene **4** was also studied by Haley *et al.*[37] Because **4** proves to be already aromatic, annelation continues and deepens the already present aromaticity.

The ring currents of the regioisomeric 16π-dibenzo[*a*,*f*]- (**11**) and dibenzo[*a*,*e*]pentalenes (**12**) were studied in detail and global antiaromaticity was found in **11**, in **12** only the core showed antiaromaticity while the terminal Clar π-sextets were characterized by aromaticity.[43–45] The spatial magnetic properties (TSNMRs) confirm the global antiaromaticity of dibenzo[*a*,*f*]pentalene **11** (Fig. 3). The dibenzo[*a*,*e*]pentalene regioisomer **12** is divided into aromatic terminal phenyl rings and an antiaromatic core, however, there is no global antiaromaticity as suggested but there is a weak counter-paratropic current loop in the core pentalene rings.[43] The corresponding ICSS (−0.5 ppm) and ICSS (−0.1 ppm) are more pronounced than the expected inner parts of the deshielding belts – therefore antiaromatic contributions to the core paratropic ring current effect can be concluded. Finally, the shielding belt in **11** and the deshielding belt in **12** are crucial in characterizing dibenzo[*a*,*f*]pentalene **11** as a PAH and dibenzo[*a*,*e*]pentalene regioisomer **12** as an antiaromatic PCH.

The balance of aromaticity and antiaromaticity in the same molecule based on the magnetic criterion

The TSNMRSs of the aromatic benzo-fused 20π-indenofluorene regioisomers **4–6** and **8**, the π-extended and curved analogues **9** and **10** and the dibenzopentalene regioisomer **12** have been unequivocally assigned to be PAHs due to the clear presence of deshielding belts; however, additionally antiaromatic contributions to the ring current effect of variable size could be concluded (*vide supra*). In order to quantify the minor antiaromatic contributions beside the dominant aromatic contributions (and *vice versa*) a larger variety of compounds have been studied in the same way to thereby expand the variety to have a larger number of correlation possibilities available. Thus, in addition to the compounds just discussed, other substances **13–21** were examined in the same way (Scheme 2). The spatial magnetic properties (TSNMRS), actually the ring current effects, of **11** and **12** are given in Fig. 3, and **13–21** in Fig. 4 and 5.

Antiaromatic compounds are generally highly reactive and kinetically unstable. Thus, molecules with paratropic contributions within the same molecule are partially less stable relative to their fully aromatic relatives. A qualification of antiaromatic contributions in PAHs (and *vice versa*) is also possible

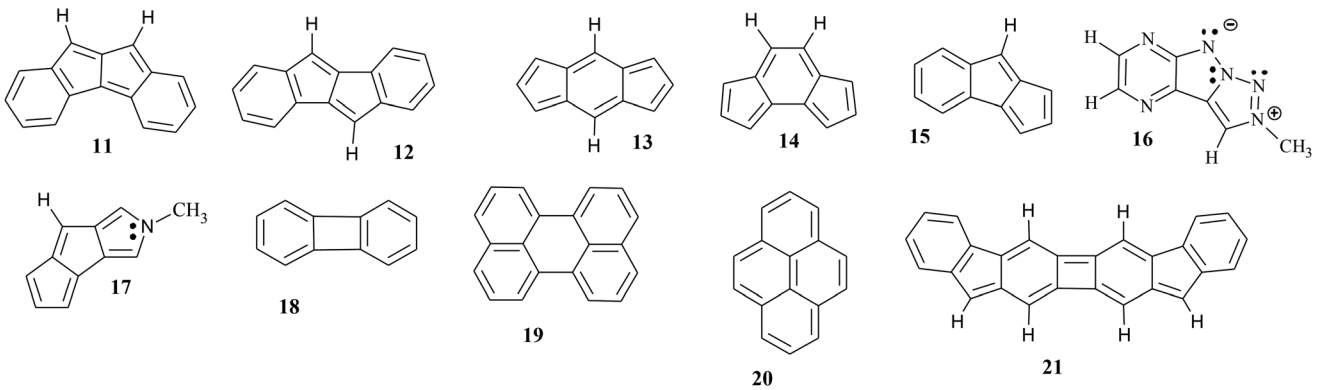

Scheme 2 Structures of studied dibenzo-pentalene regioisomers **11** and **12**, PCHs **13–15**, the N-heterocycles **16** and **17**, biphenylene **18**, perylene **19**, pyrene **20** and diindeno[2,1-*b*:2′,1′-*h*]biphenylene **21** with different numbers of annelated rings and ring sizes.

using the spatial magnetic properties (see above); a corresponding quantification would be desirable. The paratropic contributions in PAHs are only poorly evaluable using NICS-based tools because they are sum parameters of (i) the inner part of the deshielding belt of the diatropic ring current effect and (ii) the deshielding from weak counter-paratropic current loops. On the other hand, the evaluation of the diatropic ring current effect above and below the ring plane should be worthwhile, because the diatropic components present here should be able to be recorded on their own, although reduced by the existing destabilizing components of the paratropic ring current effects of varying strength. And that's what we're aiming for. We have measured the TSNMRS values and collected ICSS (+5 ppm), ICSS (+2 ppm) and ICSS (+0.5 ppm) in Table 1 for the various substances. The reduced aromaticity of the various PCHs due to antiaromatic components should be evident from this; as references the corresponding ICSS values of benzene and naphthalene are included.

There is no doubt that the indazene regioisomers **13** and **14** are antiaromatic compounds due to their ring current effects (deshielding above/below the ring plane and a complete, continuous shielding belt in-plane) and the zwitterionic polyazapentalene **16** (Fig. 4), on the other hand, is an aromatic compound;[46] the benzopentalenes **15** and **17** behave differently:[47] comparable aromatic and antiaromatic components of the ring current effects can be observed. Approximately equal proportions of aromaticity and antiaromaticity in the same molecule can be concluded. If the TSNMRS values are also used, a more precise picture emerges: the pentaleno[1,2-*c*]pyrrole **17** can be addressed as an antiaromatic PCH; the aromatic content of the phenyl moiety, compared to benzene, is greatly reduced (Table 2).

On the other hand, in the 12π benzo-pentalene **15**, the proportion is increased and sufficient to classify **15** not as an antiaromatic PCH like **17** but clearly as a mixed antiaromatic/aromatic PCH.

Table 2 TSNMRS values of benzene compared to those of **17** and **15**

TSNMRS	ICSS (+5 ppm) *blue*	ICSS (+2 ppm) *cyan*	ICSS (+0.5 ppm) *green*
Benzene	2.0 Å	3.0 Å	5.0 Å
17	1.4 Å	1.8 Å	2.5 Å
15	1.6 Å	2.0 Å	3.8 Å

The PAHs perylene (**19**), pyrene (**20**) and biphenylene (**18**) in Fig. 5 fit well into the picture drawn by the spatial magnetic properties (TSNMRSs): pyrene (**20**) with the global and two local diatropic ring currents[48] proves to be clearly aromatic, perylene (**19**), on the other hand, based on the TSNMRS representation in Fig. 5, can be electronically assigned as two naphthalene sub-units and two single bonds connecting them *via* a 6-membered ring.[49] Beside the aromatic naphthalene moieties is the central six-membered ring non-aromatic at all: the paratropic area in the centre is of exactly the same size as the deshielding belt; thus, it is only the inner part of the deshielding belt of the PAH and is in no way caused by any small residual paratropic ring current within the central part of the molecule. The TSNMRSs of biphenylene **18** also display some paratropic area in the central part of the overall clearly aromatic molecule (see the complete deshielding belt in Fig. 5). The extension of the paratropic area in the 4-membered ring (also clearly visible in Fig. 5) is significantly larger than the merely deshielding belt in pyrene (**20**). Thus, in the 4-membered ring moiety it can be concluded on a partial paratropic ring current effect in addition to the inner deshielding belt contribution; actually, the antiaromaticity of the 4-membered ring must be significant because the ring current effect of the terminal phenyl moieties proves to be tolerably reduced (Tables 1 and 3). This confirms on the basis of the magnetic criterion the results of the NICS studies reported by Gershoni-Poranne and Stanger[50] (various versions) and the ring current calculations performed by Steiner and Fowler.[51]

Table 1 Through space NMR shieldings (TSNMRSs) of polycyclic conjugated hydrocarbons (PCHs) and present (anti)aromaticity

	TSNMRSs (as various ICSSs) of aromatic moieties in the studied PCHs			
No.	ICSS (+5 ppm) *blue*	ICSS (+2 ppm) *cyan*	ICSS (+0.5 ppm) *green*	Remarks
Benzene	2.0 Å	3.0 Å	5.0 Å	—
4	1.7 Å	2.5 Å	4.4 Å	PAH
5	1.8 Å	2.6 Å	4.6 Å	PAH
6	1.6 Å	2.4 Å	4.2 Å	PAH
9	1.9 Å	2.9 Å	5.8 Å	PAH
10	—	3.2 Å	6.2 Å	PAH [central = external ICSS (−0.5/−0.1 ppm)]
8	1.5 Å	2.0 Å	3.1 Å	PAAH[a]
12	1.7 Å	2.4 Å	4.0 Å	PAAH[a]
Perylene 19	1.9 Å	3.3 Å	6.5 Å	PAH [central = external ICSS (−0.5/−0.1 ppm)]
Pyrene 20	2.5 Å	4.1 Å	7.5 Å	PAH
Biphenylene 18	1.6 Å	2.4 Å	3.8 Å	PAH
15	1.6 Å	2.0 Å	3.4 Å	PAAH[a]
17	1.4 Å	1.8 Å	2.5 Å	PAAH[a]
21	1.8 Å	2.9 Å	5.0 Å	PAH
Naphthalene	2.2 Å	3.4 Å	6.05 Å	PAH

[a] PAAH = polycyclic antiaromatic hydrocarbon.

Table 3 TSNMRS values of benzene compared to those of **18**, naphthalene, **19** and **20**

TSNMRS	ICSS (+5 ppm) *blue*	ICSS (+2 ppm) *cyan*	ICSS (+0.5 ppm) *green*
Benzene	2.0 Å	3.0 Å	5.0 Å
Biphenylene	1.6 Å	2.4 Å	3.8 Å
Naphthalene	2.2 Å	3.4 Å	6.05 Å
Perylene	2.1 Å	3.4 Å	6.4 Å
Pyrene	2.5 Å	4.1 Å	7.5 Å

The initially qualitative classification of perylene (**19**)[49] and biphenylene (**18**)[52] as PAHs without and with slight paramagnetic contributions in the central part of the molecule, respectively, can also be quantified using the ICSS values if compared to benzene or naphthalene, respectively (Table 3).

While pyrene proves to have the strongest aromaticity, the ICSS data of biphenylene are reduced as expected with respect to the benzene aromaticity due to paramagnetic contributions in the central part of the overall aromatic molecule. And the two undisturbed naphthalene molecules in perylene demonstrate with their spatial magnetic properties (TSNMRS values) the division of the molecule into two naphthalene moieties and a completely non-aromatic/non-antiaromatic 4-membered ring.

We studied also the relatively complex molecule diindeno [2,1-*b*:2′,1′-*h*]biphenylene **21** which was (heavily substituted) synthesized and studied by the group of Yao-Ting Wu in Tainan.[53] Concerning available ring current(s) in the formally aromatic 26π molecule containing two Clar's[2] π-sextets, they found out by X-ray and NICS-analysis that the six-membered rings of **21** are aromatic and the others weakly antiaromatic. Amnon Stanger,[54] who significantly further developed the NICS index,[14] also studied **21** by a $NICS(1.7)_{\pi,zz}$ approach and found a relatively strong global diatropic ring current with counter-currents in inner 5/6/4/6/5-rings; the outer 6-membered rings are diatropic. When studying the relatively complex molecule **21** he came to the final conclusion that "local aromatic indices should not be used for the full analysis of multi-ring conjugated systems",[54] and that "the local aromaticity concept should be abandoned"[54] because NICS(1) should provide misleading information.

In addition to NICS(1) values, we calculate all TSNMRSs and thereby obtain a much more comprehensive picture of the spatial magnetic properties. The TSNMRSs of **21** are given in Fig. 5, and the ICSSs above/below the center of the terminal phenyl rings are given in Table 1. First the ICSS (+5 ppm) to ICSS (+0.5 ppm) of the terminal phenyl moieties: there is no difference with the corresponding values of benzene, they are fully aromatic and the 6π aromaticity is not influenced nor distorted by the middle 5/6/4/6/5-membered rings. These rings located in the middle of the molecule also develop isolated diatropicity (of smaller size than the terminal 6π phenyls) and separated only by the inner parts of the deshielding belt of the global PAH **21**.

Lately, the validity of paratropic ring currents as tools for the characterization of antiaromatic species has been questioned Foroutan-Nejad.[55]

Conclusion

The ring current effects of a variety of Polycyclic Conjugated Hydrocarbons (PCHs) have been calculated by the GIAO perturbation method employing the nucleus independent chemical shift (NICS) concept and visualized as iso-chemical-shielding surfaces (ICSSs) of various size and direction. Thus, not only single NICS values or NICS scans (in all their versions) are used to find the global aromaticity or antiaromaticity of the PHCs or individual rings, but also the complete existing spatial magnetic properties (*i.e.* the ring current effect in the ^{1}H NMR spectrum). This means that the out of plane ICSSs in particular will be included in the indication of the spatial para- and diatropic chemical shift areas for the first time. This makes a holistic assessment of the existing PCHs based on the magnetic criterion possible: (i) the presence of deshielding belts in aromatic PCHs (or single rings in PAHs) or shielding belts in the antiaromatic analogues clearly characterizes the molecules as aromatic or antiaromatic PCHs; (ii) inner parts of the de-shielding or shielding belts can be clearly identified as such in comparison to the outer belt sizes or can be assigned as an additional part of slightly paratropic ring current effect component(s) in the corresponding ring moiety.

Conflicts of interest

The authors declare no conflicts of interest.

References

1 J. R. Platt, Classification of spectra of *cata*-condensed hydrocarbons, *J. Chem. Phys.*, 1949, **17**, 484–495.
2 E. Clar, *The Aromatic Sextet*, Wiley, 1973.
3 P. v. Ragué Schleyer, C. Maerker, A. Dransfield, H. Jiao and N. J. van Eikema Hommes, Nucleus-Independent Chemical Shifts: A simple and efficient aromaticity probe, *J. Am. Chem. Soc.*, 1996, **118**, 6317–6318.
4 C. Chen, C. S. Wannere, C. Corminboeuf, R. Puchta and P. v. Ragué Schleyer, Nucleus-independent chemical shifts (NICS) as an aromaticity criterion, *Chem. Rev.*, 2005, **105**, 3842–3888.
5 H. Fallah-Bagher-Shaidaei, C. S. Wannere, C. Corminboeuf, R. Puchta and P. v. Ragué Schleyer, Which NICS aromaticity index for planar π ring is the best?, *Org. Lett.*, 2006, **8**, 863–866.
6 A. Stanger, Nucleus-Independent Chemical Shifts (NICS): Distance dependence and revised criteria for aromaticity and antiaromaticity, *J. Org. Chem.*, 2006, **71**, 883–893.
7 A. Stanger, Obtaining relative induced ring currents quantitatively from NICS, *J. Org. Chem.*, 2010, **75**, 2281–2288.
8 A. Stanger, Reexamination of $NICS_{\pi,zz}$: Height dependence, offcenter values, and integration, *J. Phys. Chem. A*, 2019, **123**, 3922–3927.

9 J. A. Pople and K. G. Untch, Induced paramagnetic ring currents, *J. Am. Chem. Soc.*, 1966, **88**, 4811–4815.
10 D. Geuenich, K. Hess, F. Köhler and R. Herges, Anisotropy of the induced current density (ACID), a general method to quantify and visualize electronic delocalization, *Chem. Rev.*, 2005, **105**, 3758–3772.
11 T. K. Dickens and R. B. Mallion, Topological ring-currents in conjugated systems, *MATCH Commun. Math. Comput. Chem.*, 2016, **76**, 297–356.
12 D. Sundholm, M. Dimitrova and R. J. F. Berger, Current density and molecular magnetic properties, *Chem. Commun.*, 2021, **57**, 12362–12378.
13 (*a*) T. A. Keith and R. F. W. Bader, Calculation of magnetic response properties using a continuous set of gauge transformations, *Chem. Phys. Lett.*, 1993, **210**, 223–231; (*b*) T. A. Keith and R. F. W. Bader, Topological analysis of magnetically induced molecular current distributions, *J. Chem. Phys.*, 1993, **99**, 3669–3682; (*c*) T. A. Keith, Calculation of magnetizabilities using GIAO current density distributions, *Chem. Phys.*, 1996, **213**, 123–132.
14 (*a*) R. Gershoni-Poranne, C. M. Gibson, P. W. Fowler and A. Stanger, Concurrence between current density, Nucleus-Independent Chemical Shifts, and aromatic stabilization energy: The case of isomeric [4]- and [5]-phenylenes, *J. Org. Chem.*, 2013, **78**, 7544–7553; (*b*) A. Stanger, NICS – Past and present, *Eur. J. Org. Chem.*, 2020, 3120–3127.
15 S. Klod and E. Kleinpeter, Ab initio calculation of the anisotropy effect of multiple bonds and the ring current effect of arenes–application in conformational and configurational analysis, *J. Chem. Soc., Perkin Trans. 2*, 2001, 1893–1898.
16 E. Kleinpeter, Quantification and Visualization of the Anisotropy Effect in ^{1}H NMR Spectroscopy by Through-Space-NMR-Shieldings, *Annu. Rep. NMR Spectrosc.*, 2014, **82**, 115–166.
17 P. Lazzeretti, Assessment of aromaticity via molecular response properties, *Phys. Chem. Chem. Phys.*, 2004, **6**, 217–223.
18 S. Pelloni, P. Lazzeretti and R. Zanasi, Assessment of σ-diatropicity of the cyclopropane molecule, *J. Phys. Chem. A*, 2007, **111**, 8163–8169.
19 A. Stanger, What is... aromaticity: a critique of the concept of aromaticity—can it really be defined?, *Chem. Commun.*, 2009, 1939–1947.
20 E. Kleinpeter, A. Lämmermann and H. Kühn, The anisotropic effect of functional groups in ^{1}H NMR spectra is the molecular response property of spatial NICS, *Org. Biomol. Chem.*, 2011, **9**, 1098–1111.
21 E. Kleinpeter and A. Koch, The anisotropic effect of functional groups in ^{1}H NMR spectra is the molecular response property of spatial NICS – The frozen conformational equilibria of 9-arylfluorenes, *Tetrahedron*, 2011, **67**, 5740–5743.
22 E. Kleinpeter, S. Klod and A. Koch, Visualization of through space NMR shieldings of aromatic and anti-aromatic molecules and a simple means to compare and estimate aromaticity, *J. Mol. Struct.: THEOCHEM*, 2007, **811**, 45–60. and references therein.
23 E. Kleinpeter, A. Schulenburg, I. Zug and H. Hartmann, The interplay of thio(seleno)amide/vinylogous thio(seleno) amide "resonance" and the anisotropic effect of thiocarbonyl and selenocarbonyl functional groups, *J. Org. Chem.*, 2005, **70**, 6592–6602.
24 (*a*) E. Kleinpeter and A. Koch, Stable Carbenes or Betaines?, *Eur. J. Org. Chem.*, 2018, 3114–3121; (*b*) E. Kleinpeter and A. Koch, Is the term "Carbene" justified for *remote* N-heterocyclic carbenes (*r*-NHCs) and abnormal N-heterocyclic carbenes (*a*-NHCs/MICs)?, *Tetrahedron*, 2019, **75**, 1549–1554; (*c*) E. Kleinpeter and A. Koch, The ^{13}C chemical shift and the anisotropy effect of the carbene electron-deficient centre: Simple means to characterize the electron distribution of carbenes, *Magn. Reson. Chem.*, 2020, **58**, 280–292; (*d*) E. Kleinpeter and A. Koch, Bent allenes or di-1,3-betaines – An answer given on the magnetic criterion, *J. Phys. Chem. A*, 2020, **124**, 3180–3190; (*e*) E. Kleinpeter and A. Koch, Intramolecular carbene stabilization *via* 3c,2e bonding on basis of the magnetic criterion, *Tetrahedron*, 2021, **95**, 132357; (*f*) E. Kleinpeter and A. Koch, Quantification of σ-acceptor and π-donor stabilization in O, S and Hal analogues of N-Heterocyclic Carbenes (NHCs) on the magnetic criterion, *J. Phys. Chem. A*, 2021, **125**, 7235–7245; (*g*) E. Kleinpeter and A. Koch, Phosphorus stabilization of the carbene function in *P*-analogues of non-cyclic carbenes, N- heterocyclic carbenes and cyclic (alkyl)-(amino)-carbenes – An assessment on basis of geometry, ^{13}C, ^{31}P chemical shifts and the anisotropy effects of the carbene electron deficient centres, *Tetrahedron*, 2022, **121**, 132923.
25 E. Kleinpeter and A. Koch, Carbones – a classification on the magnetic criterion, *Chem. – Asian J.*, 2023, **18**, e202300826.
26 A. Artigas, D. Hagebaum-Reignier, Y. Carissan and Y. Coquerel, Visualizing electron delocalization in contorted polycyclic aromatic hydrocarbons, *Chem. Sci.*, 2021, **12**, 13092–13100.
27 M. J. Frisch, G. W. Trucks, H. B. Schlegel, G. E. Scuseria, M. A. Robb, J. R. Cheeseman, G. Scalmani, V. Barone, B. Mennucci and G. A. Petersson, *et al.*, *Gaussian 09, Revision D.01*, Gaussian, Inc., Wallingford, CT, 2009.
28 (*a*) R. Ditchfield, Self-consistent perturbation theory of diamagnetism I. A gauge- invariant LCAO method for N.M.R. chemical shifts, *Mol. Phys.*, 1974, **27**, 789–807; (*b*) G. W. Cheeseman, T. A. Trucks and M. J. Keith, A comparison of models for calculating nuclear magnetic shielding tensors, *J. Chem. Phys.*, 1996, **104**, 5497–5509.
29 A. D. Becke, Density-functional thermochemistry. III. The role of exact exchange, *J. Chem. Phys.*, 1993, **98**, 5648–5652.
30 C. Lee, W. Yang and R. G. Parr, Development of the Colle-Salvetti correlation-energy formula into a functional of the electron density, *Phys. Rev. B: Condens. Matter Mater. Phys.*, 1988, **37**, 785–789.

31 B. Miehlich, A. Savin, H. Stoll and H. Preuss, Results obtained with the correlation energy density functionals of Becke and Lee, Yang and Parr, *Chem. Phys. Lett.*, 1989, **157**, 200–206.

32 The lattice points ("*ghost atoms*") should be sensor points only without energy contribution in the present calculations. Only if DFT or HF calculations are applied is this true; in the case of electron correlation calculations, the "ghost atoms" get their own electron density and show some influence on the energy of the studied molecule. In these cases the TSNMRS surfaces are heavily distorted.

33 *SYBYL 7.3*, Tripos Inc., 1699 South Hanley Road, St Louis, Missouri 63144, USA, 2007.

34 T. Jousselin-Oba, P. E. Deal, A. G. Fix, C. K. Frederickson, C. L. Vonnegut, A. Yassar, L. N. Zakharov, M. Frigoli and M. M. Haley, Synthesis and properties of benzo-fused indeno[2,1-*c*]fluorenes, *Chem. – Asian J.*, 2019, **14**, 1737–1744.

35 Z. Zeng, X. Shi, C. Chi, J. T. López Navarrete, J. Casado and J. Wu, Pro-aromatic and antiaromatic π-conjugated molecules; an irresistible wish to be diradicals, *Chem. Soc. Rev.*, 2015, **44**, 6578–6596.

36 (*a*) C. K. Frederickson, B. D. Rose and M. M. Haley, Explorations of the indenofluorenes and expanded quinoidal analogies, *Acc. Chem. Res.*, 2017, **50**, 977–987; (*b*) C. K. Frederickson, L. N. Zakharov and M. H. Haley, Modulating paratropicity strength in diareno-fused antiaromatics, *J. Am. Chem. Soc.*, 2016, **138**, 16825–16838.

37 D. T. Chase, B. D. Rose, S. P. McClintock, L. N. Zakharov and M. M. Haley, Indeno[1,2-*b*]fluorenes: Fully conjugated antiaromatic analogues of acenes, *Angew. Chem., Int. Ed.*, 2011, **50**, 1127–1130.

38 A. G. Fix, P. E. Deal, C. L. Vonnegut, B. D. Rose, L. N. Zakharov and M. M. Haley, Indeno[2,1-*c*]fluorene: A new electron-accepting scaffold for organic electronics, *Org. Lett.*, 2013, **15**, 1362–1365.

39 Z. Majzik, N. Pavliček, M. Vilas-Varela, D. Pérez, N. Moll, E. Guitián, G. Meyer, D. Peña and L. Gross, Studying an antiaromatic polycyclic hydrocarbon adsorbed on different surfaces, *Nat. Commun.*, 2018, **9**, 1198.

40 A. Shimizu and S. Tobe, Indeno[2,1-*a*]fluorene: An air-stable *ortho*-quinodimethane derivative, *Angew. Chem., Int. Ed.*, 2011, **50**, 6906–6910.

41 A. Shimizu, R. Kishi, M. Nakano, D. Shiomi, K. Sato, T. Takui, I. Hisaki, M. Miyata and Y. Tobe, Indeno[2,1-*b*]fluorene: A 20-π-electron hydrocarbon with very low-energy light absorption, *Angew. Chem., Int. Ed.*, 2013, **52**, 6076–6079.

42 J. Liu, J. Ma, K. Zhang, P. Ravat, P. Machata, S. Avdoshenko, F. Hennersdorf, H. Komber, W. Pisula, J. J. Weigand, A. A. Popov, R. Berger, K. Müllen and X. Feng, π-Extended and curved antiaromatic polycyclic hydrocarbons, *J. Am. Chem. Soc.*, 2017, **139**, 7513–7521.

43 A. Stanger, G. Monaco and R. Zanasi, NICS-XY predictions of local, semiglobal, and global ring currents in annelated pentalenes and *s*-indazene cores compared to first- principles current density maps, *ChemPhysChem*, 2020, **21**, 65–82.

44 M. Baranac-Stojanovic' and M. Stojanovic, The effect of two types of dibenzoannulation of pentalene on molecular energies and magnetically induced currents, *Phys. Chem. Chem. Phys.*, 2019, **21**, 3250–3263.

45 J. S. Wössner, J. Kohn, D. Wassy, M. Hermann, S. Grimme and B. Besser, Increased antiaromaticity through pentalene connection in [*n*]cyclo-1,5-dibenzopentalenes, *Org. Lett.*, 2022, **24**, 983–988.

46 V. S. Gutierrez, A. Arnault, V. Ferreira, A. Artigas, D. Hagebaum-Reignier, Y. Carrisan, Y. Coquerel, M.-A. Hiebel and F. Suzenet, Synthesis, photophysical properties, and aromaticity of pyrazine-fused tetrazapentalenes, *J. Org. Chem.*, 2022, **87**, 13653–13662.

47 P. J. Mayer and G. London, Stable monoareno-pentalenes with two olefinic protons, *Org. Lett.*, 2023, **25**, 42–46.

48 (*a*) S. Fias, P. W. Fowler, J. L. Delgado, U. Hahn and P. Bultinck, Correlation of delocalization indices and current density maps in polycyclic aromatic hydrocarbons, *Chem. – Eur. J.*, 2008, **14**, 3093–3099; (*b*) R. Gershoni-Poranne and A. Stanger, The NICS-XY-Scan: Identification of local and global ring currents in multi-ring systems, *Chem. – Eur. J.*, 2014, **20**, 5673–5688.

49 D. M. Donalsson, J. M. Robertson and J. G. White, The crystal and molecular structure of perylene, *Proc. R. Soc. London, Ser. A*, 1953, **220**, 311–321.

50 R. Gershoni-Poranne and A. Stanger, The NICS-XY-Scan: Identification of local and global ring currents in multi-ring systems, *Chem. – Eur. J.*, 2014, **20**, 5673–5688.

51 E. Steiner and P. W. Fowler, Ring currents in aromatic hydrocarbons, *Int. J. Quantum Chem.*, 1996, **60**, 609–616.

52 S. Hashimoto and K. Tahara, Theoretical study on the geometry, aromaticity, and electronic properties of benzo[3,4]cyclobutathiophenes and their homologues, *J. Org. Chem.*, 2019, **84**, 9850–9858 and references therein.

53 P.-Y. Chen, Y.-C. Liu, H. Y. Hung, M. L. Pan, Y.-C. Wei, T.-C. Kuo, M.-J. Cheng, P.-T. Chou, M.-H. Chiang and Y.-T. Wu, Diindeno[2,1-*b*:2′,1′-*h*]biphenylenes: Syntheses, structural analyses, and properties, *Org. Lett.*, 2021, **23**, 8794–8798.

54 A. Stanger, The aromatic character of diindeno[2,1-*b*:2′,1′-*h*]biphenylene, *Org. Lett.*, 2022, **24**, 1243–1246.

55 C. Foroutan-Nejad, Magnetic antiaromaticity – Paratropicity does not necessarily imply instability, *J. Org. Chem.*, 2023, **88**, 14831–14835.

